Morphology of Cosmological Fields during the Epoch of Reionization

Akanksha Kapahtia
Indian Institute of Astrophysics
(Joint Astronomy Program, IISc Bengaluru)

With

Pravabati Chingangbam
(Indian Institute of Astrophysics, Bengaluru)

Stephen Appleby
(Korea Institue of Advanced Studies, Seoul)

AK, P. Chingangbam et al JCAP 2018; AK, P. Chingangbam et al arXiv:1904.06840

21cm Cosmology for Epoch of Reionization

Cosmic inflation would have amplified minute quantum fluctuations (pre-inflation) into slight density ripples of overdensity and underdensity (post-inflation)

It is these fluctuations that are the seeds of structure formation in the universe.

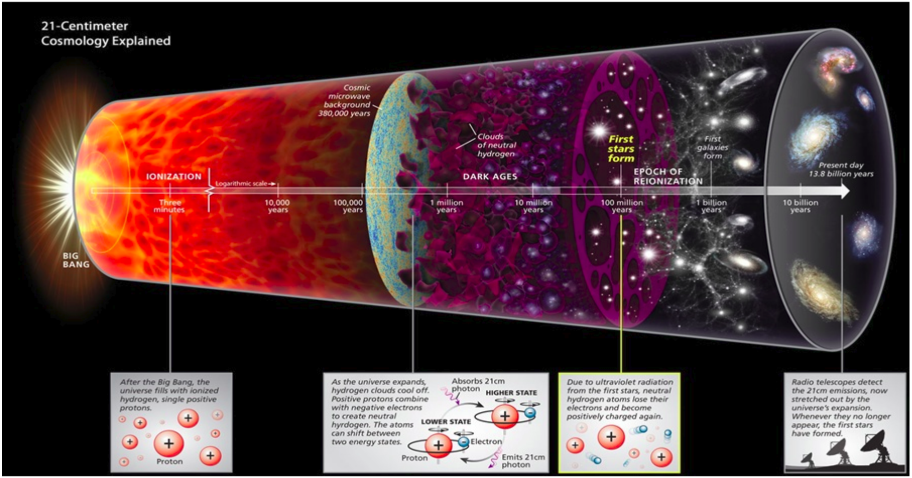

Image Credit: Roen Kelly- Discover Magazine

Observational evidence of EoR

Ly-alpha

- Spectra of distant quasars show an absorption trough.
- $x_{HI} \simeq 10^{-4}\Omega_m^{1/2}h(1+z)^{3/2}\tau_\alpha$
- Universe is highly ionized atleast till $z \simeq 6$.(Fan et.al. AnnRev.AA 2006)

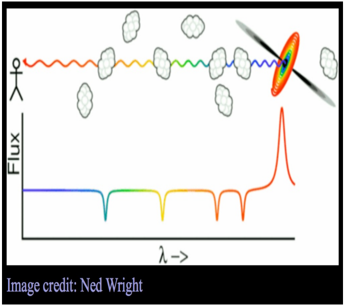

CMB

- The scattering of CMB photons induces polarizations and temperature anisotropies.
- Optical depth to last scattering, $\tau_{ls} \sim 0.054$. (Planck 2018)

The 21cm spin flip transition

Transition between $1_1 s_{1/2}$ & $1_0 s_{1/2}$

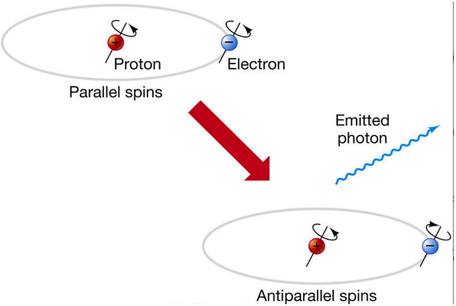

Image Credit: nrao.edu

The relative populations of hydrogen atoms in the two spin states defines the spin temperature T_s, ($T_* = 68mK, \nu_0 = 1420\ MHz$):

$$\frac{n_1}{n_0} = 3\ exp\left(\frac{-T_*}{T_s}\right)$$

$\mathbf{E} = 5.87 \times 10^{-6}\ eV$, $\mathbf{A}_{21} = 2.88 \times 10^{-15}\ sec \sim 11\ (Myr)^{-1}$

Brightness temperature

- The transfer of radiation through thermally emitting matter can be described in terms of the specific intensity:

$$\boxed{\frac{dI_\nu}{d\tau_\nu} = -I_\nu + B_\nu(T)}$$

- The temperature of a black body having the same specific intensity as I_ν is the **Brightness Temperature**.
- In RJ regime $I_\nu = \frac{2\nu^2}{c^2} kT$ and so the above equation can be written in terms of the brightness temperature, with solution:

$$\boxed{T_b'(\nu) = T_S(1 - e^{-\tau_\nu}) + T_R'(\nu) e^{-\tau_\nu}}$$

- The background radiation is usually CMB, so $T_R'(\nu) = T_\gamma(z)$

21cm Brightness Temperature

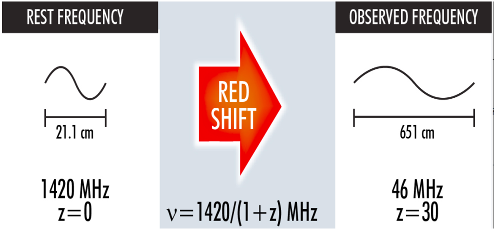

Image Credit:lunar.colorado.edu/dare/science

$$\delta T_b(\nu) = \frac{T_S - T_\gamma}{1+z}(1 - e^{-\tau_{\nu_0}}) \approx$$

$$27 x_{HI}(1+\delta_{nl})\left(\frac{H}{dv_r/dr + H}\right)\left(1 - \frac{T_\gamma}{T_S}\right)\left(\frac{1+z}{10}\frac{0.15}{\Omega_M h^2}\right)^{1/2}\left(\frac{\Omega_b h^2}{0.023}\right) \text{mK}$$

Spin Temperature

$$\delta T_b(\nu) \propto x_{HI}\ (1 + \delta_{nl})\ \left(1 - \frac{T_\gamma}{T_S}\right)$$

$\delta T_b < 0$ if $T_s < T_\gamma$: absorption
$\delta T_b > 0$ if $T_s > T_\gamma$: emission
$\delta T_b = 0$ if $T_s = T_\gamma$: No signal

Three competing processes determine T_s:

1. Absorption of CMB photons(and stimulated emission by CMB photons)
2. Collisions with other hydrogen atoms, free electrons, and protons
3. Scattering of Lyman alpha photons (Wouthuysen-Field Effect)

$$T_s^{-1} = \frac{T_\gamma^{-1} + (x_c + x_\alpha) T_k^{-1}}{1 + x_c + x_\alpha}$$

Evolution of T_s and δT_b:Models

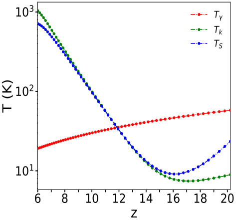

$\zeta \sim 17$ (Fid)
$\zeta_X \sim 10^{56}$

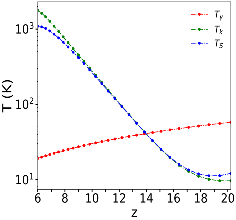

$\zeta \sim 10.9$
$\zeta_X \sim 10^{56}$

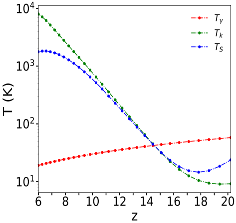

(Fid)
$\zeta_X \sim 10^{57}$

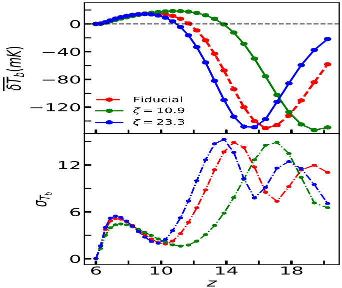

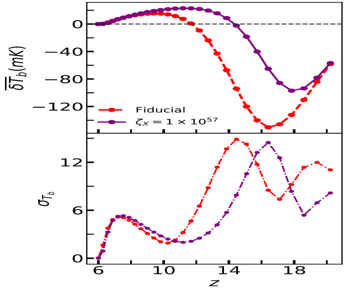

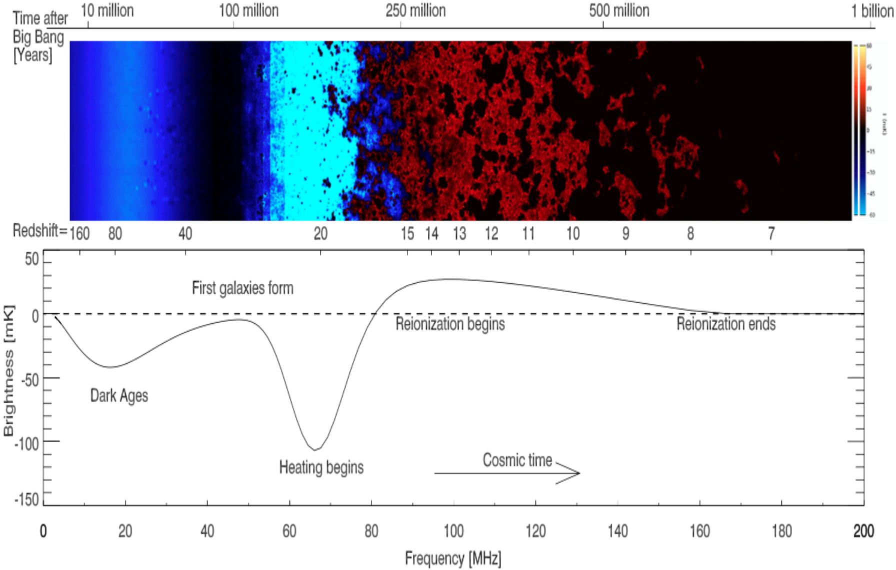

Credit:Pritchard and Loeb (2012)

Observations of the 21cm brightness temperature

There are two ways the signal is detected:

- **Global Signal**:EDGES,LEDA,DARE
- **Fluctuations**:GMRT,LOFAR,SKA,PAPER

Observational Challenge: Foregrounds are 5 orders of magnitude greater than the signal

- **Power spectrum $\rightarrow$ advantageous for observations.**
- **Fields are highly non-Gaussian $\rightarrow$ methods to include higher n-point statistics.**
- **Analyzing the morphology in real space $\rightarrow$ disadvantage as large sky volume is required for analysis.**
- **We use simulations to develop the method and make predictions for physical models.**

Morphology of cosmological fields

- **Cosmological fields** are random fluctuation fields in 2 or 3 dimensional space.
- **Excursion set**: all spatial points with field values higher than or equal to a chosen threshold.
- In 2D, boundaries form closed contours enclosing **connected regions** or **holes**.

Betti Numbers: Topological quantities

n_c = **no of connected regions** n_h = **no of holes**

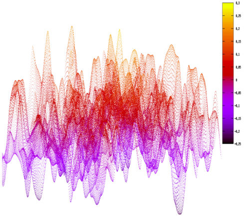

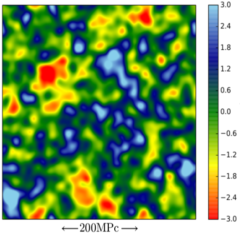

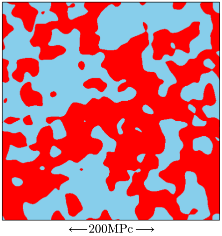

Tensor Minkowski Functionals in 2D space

Alesker 1997, Hug 2008, Beisbart et al 2002, Schroeder-Turk et al 2011

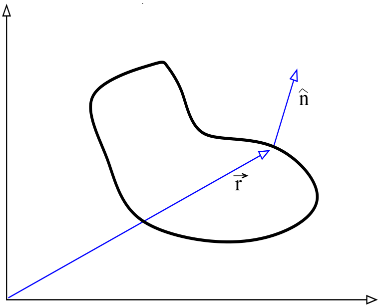

$$W_0^m \;=\; \int \vec{r}^{\,m} \;\; \mathrm{d}a$$

$$W_1^{m,n} \;=\; \int_C \vec{r}^{\,m} \otimes \hat{n}^n \;\; \mathrm{d}\ell$$

$$W_2^{m,n} \;=\; \int_C \vec{r}^{\,m} \otimes \hat{n}^n \; \kappa \;\; \mathrm{d}\ell$$

$$\kappa \;\equiv\; \text{local curvature}$$

$$(\,\vec{x} \otimes \vec{y}\,)_{ij} \;\equiv\; \frac{1}{2}(\,x_i y_j + x_j y_i\,)$$

$$m + n \leq 2$$

Scalar Minkowski Functionals : $m = 0, \; n = 0$

$$W_0 = \int \mathrm{d}a \longrightarrow \text{area}$$

$$W_1 = \int_C \mathrm{d}\ell \longrightarrow \text{contour length}$$

$$W_2 = \int_C \kappa \;\; \mathrm{d}\ell \longrightarrow \text{genus}$$

Cosmological application: Gott 1990

Tensor Minkowski Functionals: $W_1^{1,1}, W_1^{0,2}, W_2^{1,1}, W_2^{0,2}$

$$W_2^{1,1} = \int_C \vec{r} \otimes \hat{n} \; \kappa \;\; \mathrm{d}\ell = \int_C \hat{T} \otimes \hat{T} \;\; d\ell$$

$$\kappa = |d\hat{T}/d\ell|$$

(**Schroeder-Turk et al 2011, Chingangbam,KP Yogendran et al 2017**)

Translation invariant

Gives the size and shape information of the curve :

$$Trace(W_2^{1,1}) = \int_C \mathrm{d}\ell$$

Shape and Alignment measure using $W_2^{1,1}$

Single Curve:

$$W_2^{1,1} \longrightarrow \lambda_1, \lambda_2, \quad \lambda_1 < \lambda_2$$
$$\beta \equiv \frac{\lambda_1}{\lambda_2}$$
$$0 \leq \beta \leq 1$$

Many curves: :

$$\bar{\beta} \equiv \left\langle \frac{\lambda_1}{\lambda_2} \right\rangle$$

Average over all curves $\longrightarrow \left\langle W_2^{1,1} \right\rangle \longrightarrow \Lambda_1, \Lambda_2$

$$\alpha \equiv \frac{\Lambda_1}{\Lambda_2}, \qquad 0 \leq \alpha \leq 1$$

Shape and Alignment measure using $W_2^{1,1}$

β:intrinsic shape of each curve

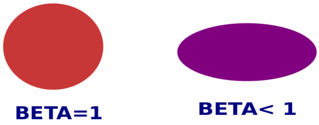

α:relative alignment of many curves

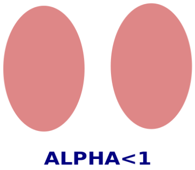

Simulating EoR

Messinger et. al., 2010

- The brightness temperature field was generated using the publicly available code `21cmFAST`.
- Uses a combination of the excursion set and perturbation theory to generate full 3D realizations of:
  - Evolved density Field
  - Ionization field - ζ and T_{vir}
  - Spin temperature field - ζ_X and T_{vir}
  - Brightness temperature field

Simulation

- Simulated δT_b, T_s, δ_{nl} and x_{HI}.
- Box size $= 200$ Mpc, resolution $= 512^3$ grid.
- Combinations of ζ and T_{vir} to correspond to reionization ending at $z \approx 6$, $\tau_{re} = 0.054$ (**PLANCK 2018**).

Morphology of fields during EoR

Physical questions

- How is the shape of structures related to the underlying physics of EoR?
- To study the morphology of δ_{nl}, T_s and x_{HI}, and see how the morphology is reflected in δT_b.
- To discriminate models of reionization
- To trace ionization and heating history of the IGM

Quantities of interest: Single curve

- $\lambda_1, \lambda_2 \longrightarrow$ Eigenvalues of W_1
- $\beta^{ch} \equiv \lambda_1/\lambda_2$
- $r^{ch} \equiv (contour\ length)/(2\pi)$
- $n_c(\nu), n_h(\nu) \longrightarrow$ Betti Numbers at a given ν

Average quantities at each threshold, ν

$$\overline{\lambda}_{i,\mathrm{x}}(\nu) \equiv \frac{\sum_{j=1}^{n_\mathrm{x}(\nu)} \lambda_{i,\mathrm{x}}(j)}{n_\mathrm{x}(\nu)}$$

$$\overline{r}_\mathrm{x}(\nu) \equiv \frac{\sum_{j=1}^{n_\mathrm{x}(\nu)} r_\mathrm{x}(j)}{n_\mathrm{x}(\nu)}$$

$$\overline{\beta}_\mathrm{x}(\nu) \equiv \frac{\sum_{j=1}^{n_\mathrm{x}(\nu)} \beta_\mathrm{x}(j)}{n_\mathrm{x}(\nu)}$$

Isotropic Gaussian random field

- The analytical forms for scalar Minkowski functionals (**Tomita 1986, Schmalzing:1998**) and α (**Chingangbam, Yogendran et al.:2017**)for Gaussian random fields is known .
- Their variation with threshold is same for a gaussian random field, irrespective of it's power spectrum.
- However, their amplitude depends upon σ_0 (standard deviation) and σ_1 (standard deviation of the field derivative).
- The variation of Betti numbers is sensitive to the power spectrum (**Park et al. 2013, Pranav 2018**) and their analytical forms is not known.
- The analytical form for variation of β is not known but it is sensitive to power spectrum.
- r^{ch} gives a measure of perimeter of individual curves. It is sensitive to power spectrum of the field.

Isotropic Gaussian random field

On varying ν from top to bottom:

- Isolated small connected regions around the highest peaks of the field and their number gradually increases
- Some of these small connected regions merge thereby decreasing their number.
- Connected regions all merge to form a single connected region with holes puncturing it which shrink in size and disappear as we go lower in threshold.

(Image Credit:Feldbrugge and Engelen,University of Groningen (2012))

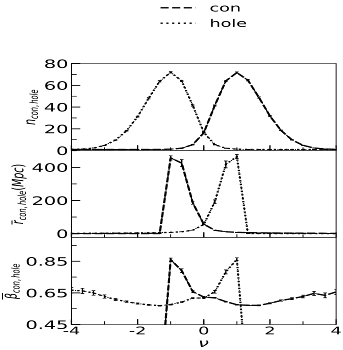

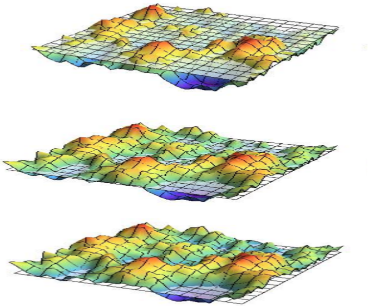

Redshift Evolution of average quantities

Condense the ν dependence to get a single quantity at each redshift

$$
\begin{aligned}
N_{\rm x}(z) &\equiv \int_{\nu_{\rm low}}^{\nu_{\rm high}} {\rm d}\nu\, n_{\rm x}(\nu, z) \\
\lambda_{i,{\rm x}}^{\rm ch}(z) &\equiv \frac{\int_{\nu_{\rm low}}^{\nu_{\rm high}} {\rm d}\nu\, n_{\rm x}(\nu, z)\bar{\lambda}_{i,{\rm x}}(\nu)}{N_{\rm x}(z)} \\
r_{\rm x}^{\rm ch}(z) &\equiv \frac{\int_{\nu_{\rm low}}^{\nu_{\rm high}} {\rm d}\nu\, n_{\rm x}(\nu, z)\bar{r}_{\rm x}(\nu)}{N_{\rm x}(z)} \\
\beta_{\rm x}^{\rm ch}(z) &\equiv \frac{\int_{\nu_{\rm low}}^{\nu_{\rm high}} {\rm d}\nu\, n_{\rm x}(\nu, z)\bar{\beta}_{\rm x}(\nu)}{N_{\rm x}(z)}
\end{aligned}
$$

$\nu_{\rm high}$ and $\nu_{\rm low}$ can be suitably chosen based on physical interpretation.

Morphology of δ_{nl}

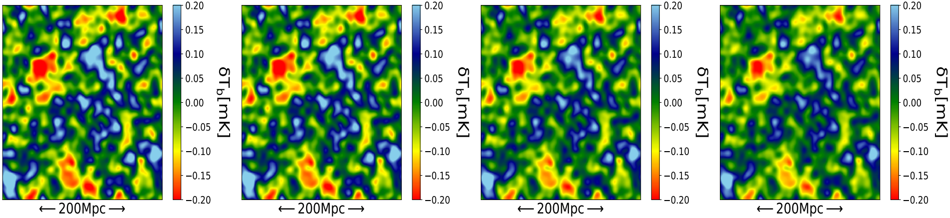

z=15.73 z=16.41 z=18.60 z=20.22

Peaks grow **BUT** at the cost of valleys

Morphology of δ_{nl}

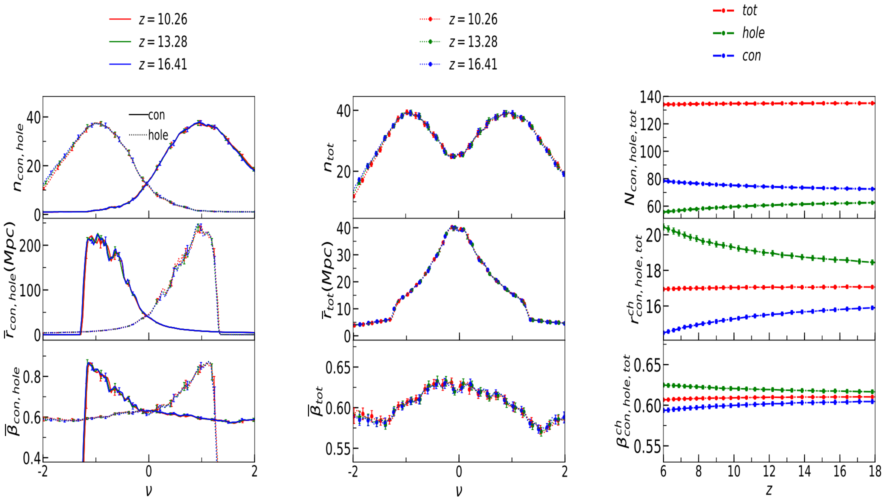

Morphology of x_{HI} field

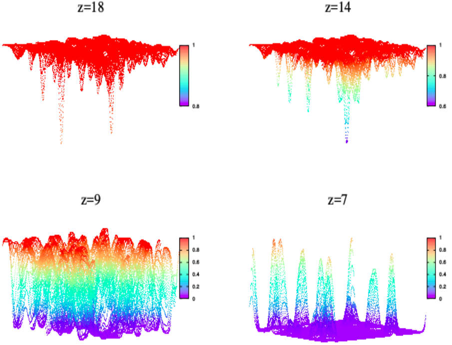

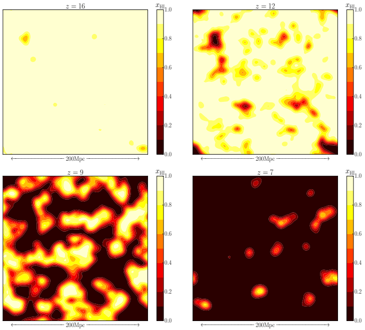

To define a connected region or hole as neutral or ionized:

Holes: If $\nu_{max} > 0$ then $\nu_{high} = 0$
Connected Regions: If $\nu_{min} < 0$ then $\nu_{low} = 0$

Morphology of x_{HI} field : Progress of ionization

- The rate of Formation of sources
- The rate of growth of Bubbles
- The rate of mergers of Bubbles

$z_{frag} \longrightarrow$ Rate of source formation=Merger rate of Bubbles

$z_{0.5} \longrightarrow N_c = N_h$

$z_e \longrightarrow N_c$ starts decreasing

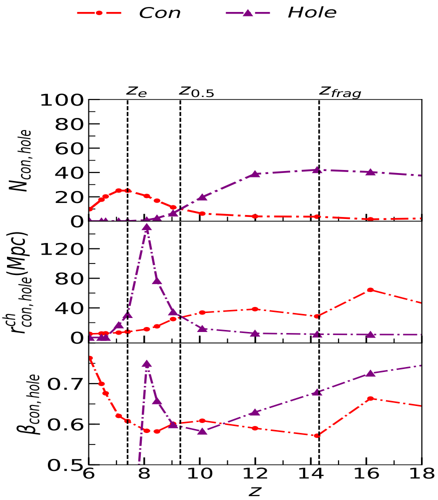

Morphology of x_{HI} field: Model Comparison

$$\zeta f_{coll}(x, z, R) \geq 1$$

Number of ionizing photons $>$ number of neutral hydrogen atoms

- *Fiducial model*: $\zeta = 17.5$, $\zeta_X = 2 \times 10^{56}$, $T_{vir} = 3 \times 10^4$ K
- Fiducial model with $\zeta = 10.9$, $T_{vir} = 1 \times 10^4$ K
- Fiducial model with $\zeta = 23.3$, $T_{vir} = 5 \times 10^3$ K

$$\zeta f_{coll}(x, z, R) \geq 1 + \overline{n}_{rec}(x, z, R)$$

Morphology of x_{HI} field: Model Comparison

Low $T_{vir} \rightarrow$ Less efficient but more numerous sources –Frequent mergers

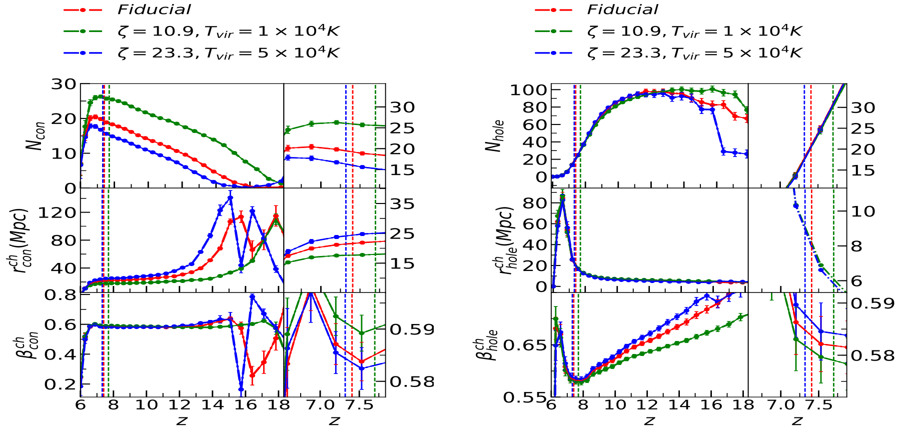

Morphology of T_s field

$$\boxed{\mathbf{T_s^{-1} = \frac{T_\gamma^{-1} + (x_c + x_\alpha)T_k^{-1}}{1 + x_c + x_\alpha}}}$$

- Fluctuations in x_c at these redshifts can be ignored.
- Therefore only fluctuations in x_α and T_k determine T_s fluctuations.
- Before X-ray heating, $T_k \propto 1/(1+z)^{-2} \rightarrow$ no fluctuations in T_k, only fluctuations in x_α will determine the fluctuations in T_s.
- If x_α is high, T_S is closer to T_K than it is to T_γ, hence T_s will be closer to T_K evolution in such regions.
- $x_\alpha \propto (1+z)^{-1}\ J_\alpha$ which is the $Ly-\alpha$ background flux which depends directly upon the rate of appearance of $Ly-\alpha$ sources.
- Soon x_α will saturate and highest density regions will now host X-ray efficient sources $\rightarrow$ T_k is now fluctuating component and determines the fluctuations in T_s.

Highest Density regions have higher x_α and hence lower T_s The same regions will be the first places where X-ray sources will appear at later times

Flipping between a valley and a peak

Density

T_s

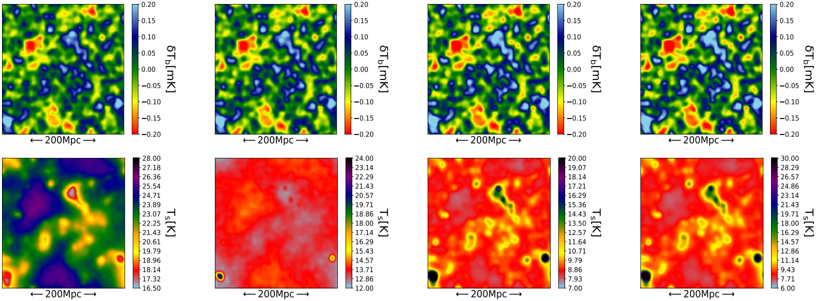

z=20.22 z=18.60 z=16.41 z=15.73

Morphology T_s Field : Model Comparison

$\zeta_X \rightarrow$ Number of X-ray photons produced per solar mass

Lower $T_{vir} \rightarrow$ Less efficient sources

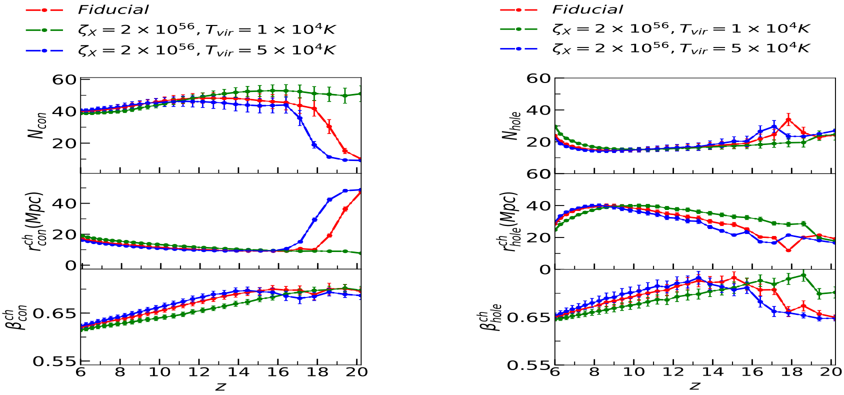

Morphology T_s Field : Model Comparison

$\zeta_X \rightarrow$ Number of X-ray photons produced per solar mass

Lower ζ_X correspond to less efficient sources

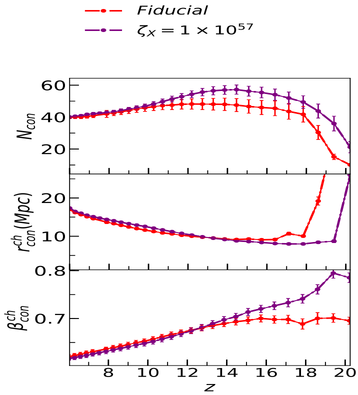

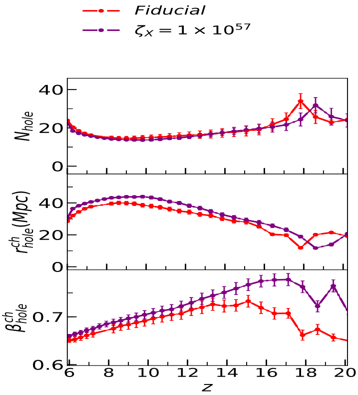

Morphology of δT_b Field

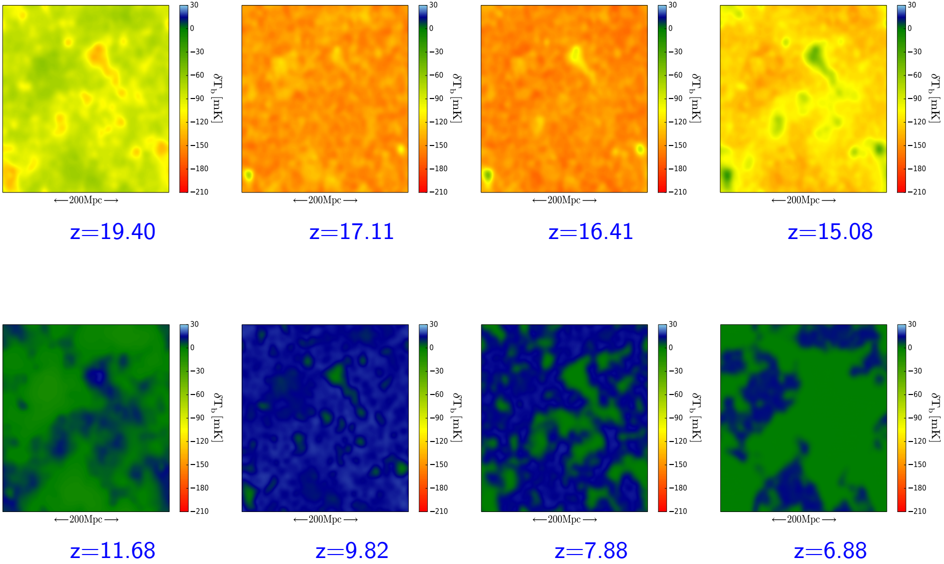

Morphology of δT_b Field

Regime 1:
$\mathbf{z} > \mathbf{z_{tr}}$
T_s & δ_{nl}

Regime 2:
$\mathbf{z_{frag}} < \mathbf{z} < \mathbf{z_{tr}}$
T_s & xHI with T_s dominating

Regime 3:
$\mathbf{z_{EoR}} < \mathbf{z} < \mathbf{z_{frag}}$
T_s & xHI with xHI dominating

Regime 4: $\mathbf{z} < \mathbf{z_{EoR}}$ T_b *follows* x_{HI}

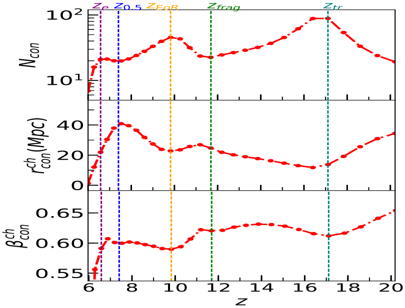

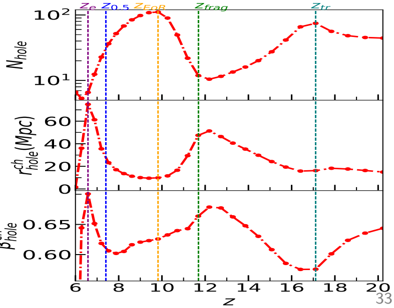

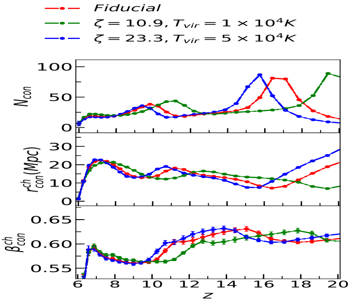
Fiducial
$\zeta = 10.9, T_{vir} = 1 \times 10^4 K$
$\zeta = 23.3, T_{vir} = 5 \times 10^4 K$
N_{con}
$r^{ch}_{con}(Mpc)$
β^{ch}_{con}
z

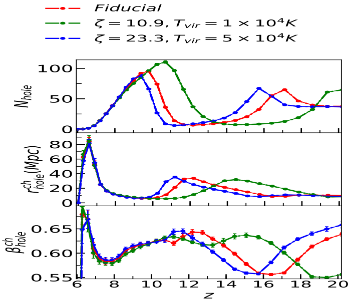
Fiducial
$\zeta = 10.9, T_{vir} = 1 \times 10^4 K$
$\zeta = 23.3, T_{vir} = 5 \times 10^4 K$
N_{hole}
$r^{ch}_{hole}(Mpc)$
β^{ch}_{hole}
z

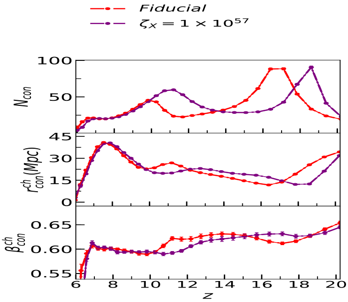
Fiducial
$\zeta_X = 1 \times 10^{57}$
N_{con}
$r^{ch}_{con}(Mpc)$
β^{ch}_{con}
z

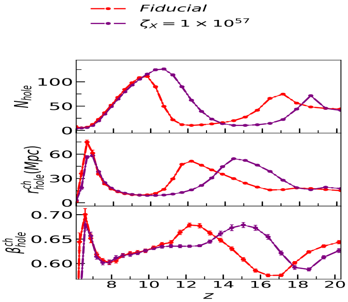
Fiducial
$\zeta_X = 1 \times 10^{57}$
N_{hole}
$r^{ch}_{hole}(Mpc)$
β^{ch}_{hole}
z

Summary

Kapahtia, Chingangbam et al (arXiv:1904.06840)-Under review

Model	z_{frag}	$z_{0.5}$	z_e	z_{re}	τ_{re}
Fiducial	~ 11.69	~ 7.407	~ 6.58	~ 6.28	~ 0.054
$T_{vir} = 1 \times 10^4 K$	~ 13.857	~ 7.698	~ 6.58	~ 6.00	~ 0.058
$T_{vir} = 5 \times 10^4 K$	~ 11.194	~ 7.32	~ 6.58	~ 6.00	~ 0.052
$\zeta_X = 1 \times 10^{57}$	~ 12.73	~ 7.5	~ 6.58	~ 6.28	~ 0.034
Recombination	~ 12.2	~ 6.8	–	< 6.00	

Model	$r^{ch}_{z_{0.5}}$ (Mpc)	z_{EoR}	$\bar{x}^{EoR}_{HI}$	z_{tr}
Fiducial	$\sim 20.5 \pm 0.78$	~ 8.7	~ 0.73	~ 17.11
$T_{vir} = 1 \times 10^4 K$	$\sim 15 \pm 0.424$	~ 9.1	~ 0.71	~ 19.4
$T_{vir} = 5 \times 10^4 K$	$\sim 22.5 \pm 0.96$	~ 8.6	~ 0.77	~ 15.7
$\zeta_X = 1 \times 10^{57}$	$\sim 20 \pm 0.689$	~ 9.12	~ 0.77	~ 18.6

Conclusion

- The number, size and shape of structures of excursion set of the fields exhibit clear evolution as a function of redshift.
- This evolution gives the important time and length scales of EoR
- This allows us to discriminate different EoR models

Ongoing and future Work

- Sensitivity and signal to noise measures of Minkowski functionals for SKA like interferometers.
- Performing Bayesian analysis to obtain constraints on different models of reionization
- Extension to Minkowski tensors in 3-D.